Michael Unger, Johann Berger, Bjoern Gerold and Andreas Melzer*

Robot-assisted Ultrasound-guided Tracking of Anatomical Structures for the Application of Focused Ultrasound

Abstract: High intensity focused ultrasound is used as a surgical tool to treat completely non-invasively several diseases. Examples of clinical applications are uterine fibroids, prostate cancer, thyroid nodules, and varicose veins. Precise targeting is key for improving the treatment outcome. A method for an automated, robot-assisted tracking system was developed and evaluated. A wireless ultrasound scanner was used to acquire images of the target, in this case, a blood vessel. The active contour approach by Chan and Vese was used to segment and track while moving the scanner along the target structure with a collaborative robotic arm. The performance was assessed using a custom made Agar phantom. The mean tracking error, which is defined as the remaining distance of the lesion to the images' centre line, was 0.27 mm ± 0.18 mm.

Keywords: robotic arm, HIFU, FUS, segmentation, tracking

https://doi.org/10.1515/cdbme-2020-3032

1 Introduction

High intensity focused ultrasound (HIFU) or focused ultrasound (FUS) allows to precisely deliver energy into the human body. The induced thermal and mechanical effects enable the treatment of a variety of pathologies, like the ablation of benign and malign tumours [1, 2]. Furthermore, heating tumour cells to non-lethal temperatures in the range of 41 °C to 46 °C causes a beneficial radio-sensitizing effect for adjuvant treatment to radiation therapy [3, 4].

For the application of FUS specialized devices are needed depending on the location of the treatment target. FUS devices range from fully integrated MRI-based solutions for MR-guided interventions to stand-alone US-guided HIFU systems. In the case of adjuvant radiotherapy, only mobile systems that can be used in the radiation control area are suitable.

Positioning the FUS transducer requires high precision to ensure the treatment focus is targeted to the correct tissue structures according to the treatment plan. Robotic systems provide sufficient, precision, flexibility, and reproducibility to fulfil these requirements. Surgical robots have been used to compensate small movements of patients in orthopaedic surgery [5]. Schweikard et al. demonstrated the compensation of respiratory motion using robotic radiosurgery [6]. Xiao et al. used developed active tracking for the application of focussed ultrasound using a robotic arm and MR guidance [7]. Chanel et al. developed a robotic HIFU system for the application of US-guided FUS while tracking the target [8].

This paper presents a validation study for the automated tracking of a vessel structure in ultrasound images to adjust the position of the robot-guided transducer. A collaborative robotic system was used to move the ultrasound probe along the target structure while correcting the lateral position to align the target to the centre of the image, enabling an automated tool-positioning.

2 Material and Methods

A system consisting of a robotic arm (KUKA LBR Med, Kuka AG, Germany) was used for the positioning of a wireless ultrasound scanner (Clarius L7, Clarius Inc., Canada). A custom made phantom has been used to evaluate the automatic tracking. The prototypical setup is shown in Figure 1. A software tool to semi-automatically segment structures of interest was implemented in C++.

For the tracking of anatomical structures, a phantom with an artificial blood vessel was manufactured. Agar gel with a

***Corresponding author: Andreas Melzer:** Innovation Center Computer Assisted Surgery, Semmelweisstr. 14, Leipzig, Germany, e-mail: andreas.melzer@medizin.uni-leipzig.de
Johann Berger, Michael Unger: Innovation Center Computer Assisted Surgery, Leipzig, Germany
Bjoern Gerold: Theraclion SA, Malakoff, France

concentration of 4 % w/v m in water doped with 10 % w/v sodium chloride was prepared to mimic the tissue.

Segmentation Algorithm

The segmentation of structures in medical images is a common problem. Various challenges present a hurdle to be overcome when segmenting B-mode ultrasound images [9].

Active contours based on level-sets provide segmentation schemes to partition the image domain into different regions. In contrast to edge-based schemes such as *classical Snakes*, region-based methods tend to be less sensitive to noise [10]. Active contours methods deform a contour iteratively to fit the represented visual information. Various approaches were proposed to optimize the partitioning process. We used the concept of Chan and Vese [11], which minimizes a global energy function to detect objects whose boundaries are not necessarily defined and for which the more common active contour models are not applicable.

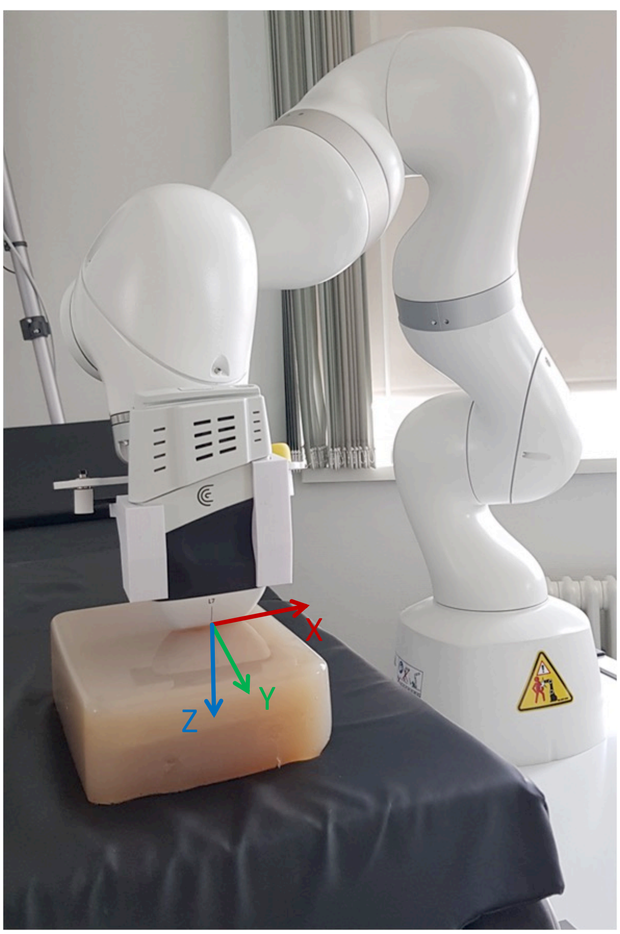

Figure 1: Setup of the evaluation. The Clarius L7 wireless ultrasound scanner was attached to the KUKA LBR Med robotic arm. An agar phantom with an artificial anatomical structure to evaluate the tracking performance.

A tool to acquire US images via network using the Clarius-SDK (software development toolkit) provided by the vendor was implemented. The acquired images were segmented using the active contour implementation of Lankton [12]. The source code was modified to be compatible with the open computer vision toolkit (OpenCV) to perform image processing and visualize the user interface.

When provided with an image sequence, the segmentation algorithm requires an initial contour in the first image slice to perform correctly. Therefore, the user has to manually create a mask of 20-pixel diameter in the structure of interest, by clicking in the user interface. A first segmentation is calculated and its result is then used as the starting contour for subsequent images.

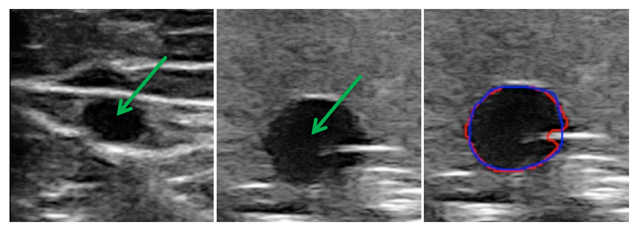

Figure 2: Ultrasound image of the great saphenous vein (left), the artificial vessel in the Agar phantom (center) and the segmentation example (right). The segmentation of the user is denoted by the blue contour and the segmentation of the algorithm is denoted by the red contour.

Robotics System Integration

To test the tracking software's performance in context with a robotic system for automated target alignment, a KUKA LBR Med was utilized to dynamically position the US scanner on an Agar-based phantom. To allow for a simple transition from ultrasound image coordinates to robot positioning movements, the scanner was attached to the robotic flange, so that the tools' x and z-axis were aligned with the x and y coordinates in the ultrasound image, respectively (Figure. 1). The phantom was prepositioned under the tool so that the simulated vein was visible in the US image. Afterward, a semi-automated application was used to advance the robot stepwise in the scanner's y-direction with a step size of 2 mm. This application was communicating with the tracking algorithm via a standard User Datagram Protocol (UDP) network connection. Hence, after each z-translation, the robot application received new positional information of the vein inside the ultrasound image from the tracking application and performed a relative translational movement in the x-direction accordingly. After each repetition of a y and x-directional movement, the current ultrasound image, the tracking position of the vessel centre in the image, as well as the ultrasound scanner's position in the robot's coordinate system were recorded.

Evaluation

For the tracking of anatomical structures, the Agar phantom with an artificial blood vessel embedded is suitable to mimic the tissue. A 10 mm polyurethane tube was placed inside the gel and removed after solidification. The remaining cavity was filled with pure ethanol and sealed with agar gel, enabling the acquisition of sufficiently contrasted ultrasound images (see Figure 2).

The segmentation performance was evaluated on a data set of the great saphenous vein acquired from the corresponding author and the artificial vein tracked by the robot. Therefore, 64 images of the GSV of the upper thigh and 50 images of each of two the artificial vessels were assessed. The images were stored for post-processing using the Digital Imaging and Communications in Medicine (DICOM) standard. The structures were segmented by two probands, experienced in image segmentation. The manual segmentation result was compared to that of the algorithm by calculating the mean of the distances between the centre of mass in each image.

The tracking performance was evaluated by moving the US scanner 2 mm perpendicular to the imaging plane, acquiring a US image, retrieving the centre of the structure and correcting the position of the US scanner along the imaging plane. The remaining error was assessed by manually segmenting the structure in the US image after the position correction and calculating the distance to the centre line of the US image.

3 Results

The segmentation error of the GSV data set was 0.47 ± 0.39 mm (mean ± std) and 0.48 ± 0.39 mm for the phantom.
No significant difference ($p < 0.05$) between the two manual segmentations was measured. The segmentation error for segmenter 1 was 0.45 ± 0.37 and 0.56 ± 0.37 for the GSV and phantom respectively. The segmentation error for segmenter 2 was 0.48 ± 0.40 and 0.41 ± 0.40 for the GSV and phantom respectively. The mean tracking error was 0.27 ± 0.18 mm and the mean segmentation time was 0.42 s.

The distribution of the segmentation and tracking error is depicted in Figure 3, the resulting trajectories of the US scanner are visualized in Figure 4.

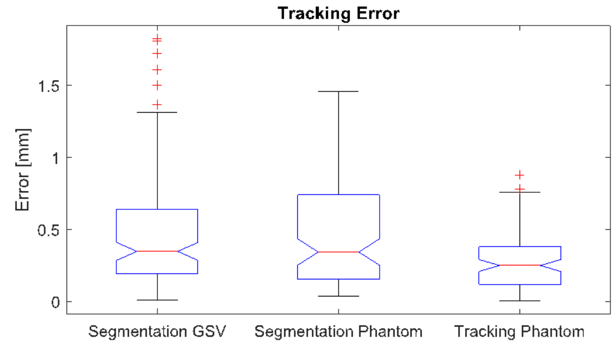

Figure 3: Distribution of the segmentation error for the GSV data set and the phantom data set and the tracking error.

4 Discussion and Conclusion

The segmentation errors for the natural and artificial veins are similar. The segmentation error of the artificial vein shows a slightly higher spread which might be caused by the lower contrast in the phantom (see Figure 2). The tissue of the phantom is much more homogeneous, although distortions can be seen at the bottom.

The tracking error of 0.27 mm is smaller than the segmentation error which originates from the calculation method. After correcting the lateral position of the US scanner the remaining error is the distance to the centre line of the image. Hence, only the horizontal component of the position is taken into account and the tracking error is less than the segmentation error. The small remaining tracking error enables the robotic system to be used even for the tracking of fine anatomical structures if the segmentation performs well.

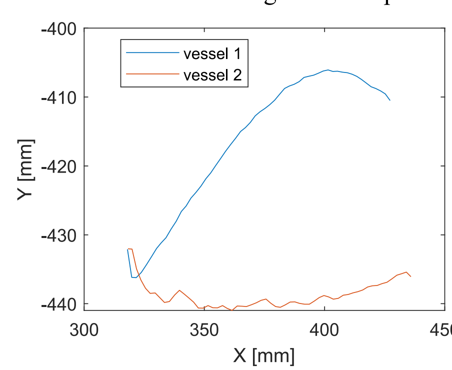

Figure 4: Trajectories of the scanner in the robot's base coordinate system. The trajectories of the two vessels differ in the xy-plane.

In its current implementation, too fast movement of the scanner may lead to lost tracking in which case the user needs to select a new initial contour.

Active contours are sensitive to parameter selection. Although no cumbersome tuning of the parameters was necessary for our use-case, this behaviour needs to be considered for the segmentation of different anatomical structures. Therefore, further assessment of the segmentation method needs to be taken into account, especially if robot-assisted US-guided tracking will be applied in further use-cases.

Author Statement

Research funding: This project has received funding from the Eurostars-2 joint programme with co-funding from the European Union Horizon 2020 research and innovation programme (grant number E!12491). Conflict of interest: Authors state no conflict of interest.

References

1. Izadifar Z, Izadifar Z, Chapman D, Babyn P (2020) An Introduction to High Intensity Focused Ultrasound: Systematic Review on Principles, Devices, and Clinical Applications. Journal of Clinical Medicine 9:460. https://doi.org/10.3390/jcm9020460

2. Barnat N, Grisey A, Gerold B, et al (2020) Efficacy and safety assessment of an ultrasound-based thermal treatment of varicose veins in a sheep model. International Journal of Hyperthermia 37:231–244. https://doi.org/10.1080/02656736.2020.1734672

3. Horsman MR, Overgaard J (2007) Hyperthermia: a Potent Enhancer of Radiotherapy. Clinical Oncology 19:418–426. https://doi.org/10.1016/j.clon.2007.03.015

4. Zhu L, Altman MB, Laszlo A, et al (2019) Ultrasound Hyperthermia Technology for Radiosensitization. Ultrasound in Medicine & Biology 45:1025–1043. https://doi.org/10.1016/j.ultrasmedbio.2018.12.007

5. Knappe P, Gross I, Pieck S, et al (2003) Position control of a surgical robot by a navigation system. In: Proceedings 2003 IEEE/RSJ International Conference on Intelligent Robots and Systems (IROS 2003) (Cat. No.03CH37453). pp 3350–3354 vol.3

6. Schweikard A, Glosser G, Bodduluri M, et al (2000) Robotic motion compensation for respiratory movement during radiosurgery. Computer Aided Surgery 5:263–277. https://doi.org/10.1002/1097-0150(2000)5:4<263::AID-IGS5>3.0.CO;2-2

7. Xiao X, Huang Z, Rube MA, Melzer A (2017) Investigation of active tracking for robotic arm assisted magnetic resonance guided focused ultrasound ablation. Int J Med Robotics Comput Assist Surg 13:n/a-n/a. https://doi.org/10.1002/rcs.1768

8. Chanel L-A, Nageotte F, Vappou J, et al (2015) Robotized High Intensity Focused Ultrasound (HIFU) system for treatment of mobile organs using motion tracking by ultrasound imaging: An in vitro study. In: 2015 37th Annual International Conference of the IEEE Engineering in Medicine and Biology Society (EMBC). pp 2571–2575

9. Meiburger KM, Acharya UR, Molinari F (2018) Automated localization and segmentation techniques for B-mode ultrasound images: A review. Computers in Biology and Medicine 92:210–235. https://doi.org/10.1016/j.compbiomed.2017.11.018

10. Cremers D, Rousson M, Deriche R (2007) A Review of Statistical Approaches to Level Set Segmentation: Integrating Color, Texture, Motion and Shape. Int J Comput Vision 72:195–215. https://doi.org/10.1007/s11263-006-8711-1

11. Chan TF, Vese LA (2001) Active contours without edges. IEEE Transactions on Image Processing 10:266–277. https://doi.org/10.1109/83.902291

12. Lankton S (2009) Sparse field methods-technical report. Georgia institute of technology